

Bicyclo[4.1.1]octanes via Strain-Storage Cyclobutanone-Alkyne Coupling and Its Enantioselective Strain-Release Transformation to Bicyclo[4.2.1]nonanes

Hanlin Yang, Lingfei Hu, Gang Lu,* Xingwei Li,* and Songjie Yu*



Cite This: *ACS Catal.* 2025, 15, 4901–4910



Read Online

ACCESS |

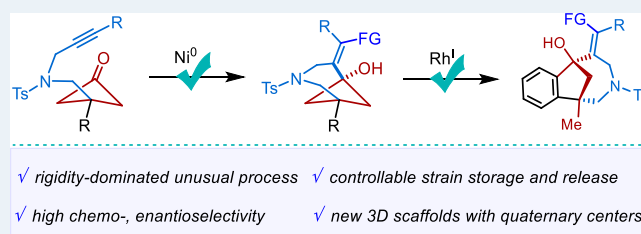
Metrics & More

Article Recommendations

Supporting Information

ABSTRACT: Three-dimensional C(sp³)-rich bicyclic scaffolds are vital saturated bioisosteres and versatile building blocks in medicinal and synthetic chemistry. Notwithstanding the importance and progress, the synthesis of bicyclo[4.1.1] and bicyclo[4.2.1] scaffolds remains challenging. Herein, we unveil a rare nickel-catalyzed strain-storage cyclobutanone-alkyne coupling to prepare various functionalized bicyclo[4.1.1]octanes. Moreover, downstream strain-release transformation of bicyclo[4.1.1] scaffolds via rhodium-catalyzed enantioselective sequential C–C activation and 1,4-rhodium shift was efficiently achieved to fuse a variety of enantioenriched bicyclo[4.2.1] scaffolds with high chemo-, diastereo-, and enantioselectivity. Mechanistic studies revealed the well-tailored spironickelabicyclic intermediate with a rigid endo-cyclic olefin favors the strain-storage cyclometalation over the common strain-release-driven β -carbon elimination.

KEYWORDS: transition metal catalysis, bicyclo[4.1.1], bicyclo[4.2.1], strain storage and release, mechanistic study



INTRODUCTION

Three-dimensional (3D) bicyclo[*n*.1.1] (*n* = 1–5) are privileged scaffolds in medicinal chemistry because of their profound bioisosteric applications to enhance the physicochemical and pharmacokinetic properties of bioactive compounds.¹ On the other hand, due to the large strain energies embedded in the 4-membered ring of bicyclo[*n*.1.1] systems, these strained 3D bicyclic molecules frequently serve as important building blocks in organic synthesis.² Thus, both aspects have led to extensive researches on designing new practical methodologies to synthesize these strained bridged bicyclic skeletons with highly structural diversity.³ Recently, radical addition to the central bond of [*n*.1.1]propellane (*n* = 1 and 3) and formal bicyclo[1.1.0]butane cycloaddition with unsaturated π -units have exhibited a wide range of applications in the construction of various bicyclo[1.1.1],⁴ bicyclo[2.1.1],⁵ bicyclo[3.1.1],⁶ and bicyclo[5.1.1]⁷ systems. However, as an integral part of bicyclo[*n*.1.1] family, bicyclo[4.1.1] scaffold⁸ was inaccessible due to the absence of reactivity-matched coupling partners. As our continuous interest in synthesis and transformation of 3D bicyclic scaffolds,⁹ we aimed to establish a unique strategy to realize bicyclo[4.1.1] scaffold synthesis and simultaneously investigate their chemical reactivity to produce new polycyclic structures and mimic potential metabolic pathways as a bioisostere.

Transition metal-catalyzed couplings of cyclobutanone derivatives with unsaturated molecules such as alkene,¹⁰ alkynes,¹¹ and allenes¹² represent an important strategy for synthesis of cyclic compounds, especially the bridged bicycles

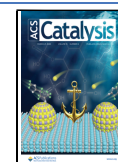
through an intramolecular coupling manner.¹³ Among the metal catalysts, nickel, being a cheap catalyst, has also exhibited a remarkable catalytic reactivity toward such couplings.¹⁴ For example, Dong reported a nickel-catalyzed intramolecular [4 + 2] coupling of cyclobutanones with allenes to form bicyclo[3.2.2] scaffolds.¹⁵ Despite this progress, to date, there exists no report on a strained scaffold using this strategy due to the primary barrier of strain-release-driven C–C cleavage via either originally proposed oxidative cyclometalation and subsequent β -C elimination¹⁶ or recent DFT-established C–C oxidative addition of cyclobutanone and successive migratory insertion (Scheme 1a, left).¹⁷ To promote nickel-catalyzed carbonyl-alkyne coupling over the facile strained C–C oxidative addition, we reckon that the alkyne-substituted cyclobutanones might be competent substrates. When bonded side-on to a nickel center, the alkyne serves as a dihapto, usually two-electron donor. The metallacyclopropanation of nickel with alkyne through strong π -backbonding into the π^* antibonding orbital of alkyne¹⁸ increases the nucleophilicity of alkyne moiety, thus finally accelerating the formal carbonyl-alkyne oxidative cyclometalation over the C–

Received: January 4, 2025

Revised: February 25, 2025

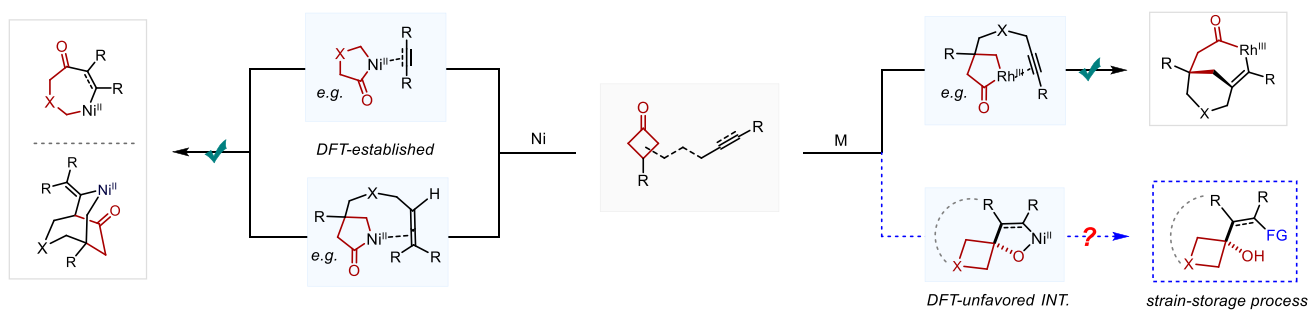
Accepted: February 27, 2025

Published: March 7, 2025

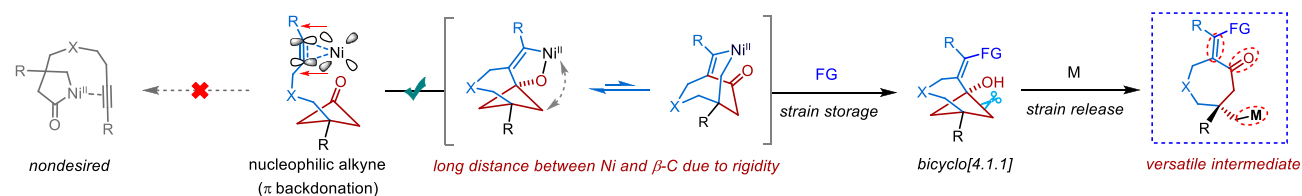


Scheme 1. Metal-Catalyzed Strain-Storage and -Release Transformations

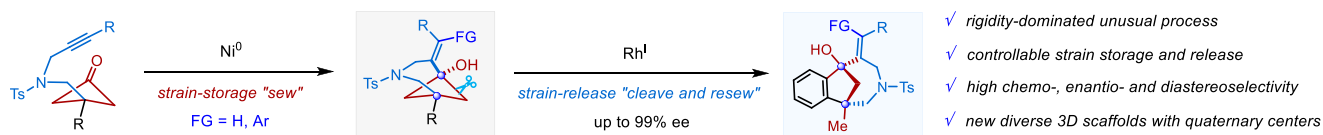
a) Metal-catalyzed strain-release transformations of cyclobutanone derivatives



b) Conceptual design for controllable strain-storage and -release process



c) Bicyclo[4.1.1] synthesis and enantioselective transformation to bicyclo[4.2.1] (this work)

Table 1. Condition Optimization^a

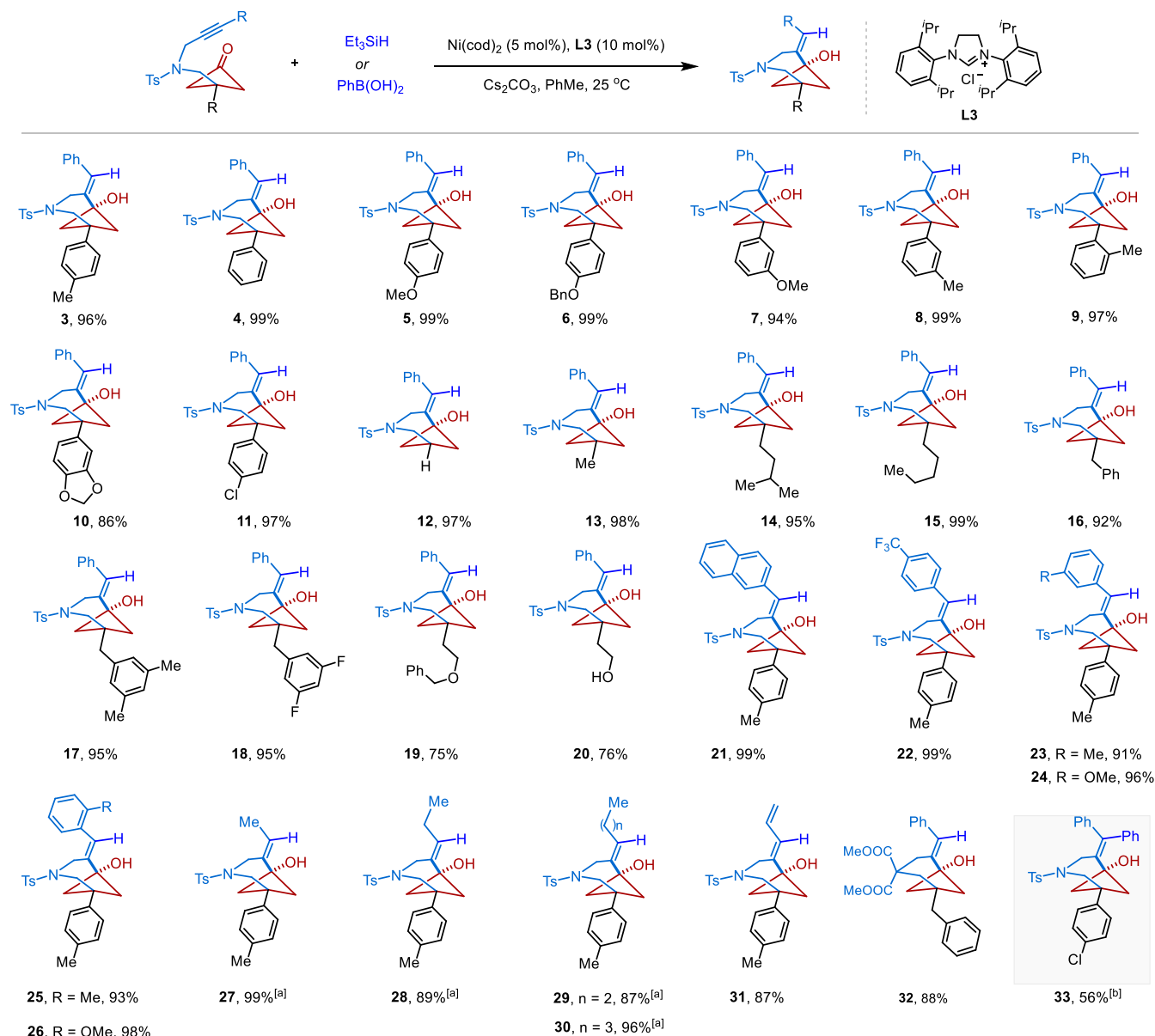
entry	Ni(cod) ₂ /mol %	ligand/mol %	[H]/equiv	solvent	base/equiv	T/°C	yield/% ^{b,c}
1	10	L1/20	Et ₃ SiH/2	PhMe	Cs ₂ CO ₃ /2	100	69
2	10	L1/20	B ₂ pin ₂ /2	PhMe	Cs ₂ CO ₃ /2	100	45
3	10	L1/20	HBpin/2	PhMe	Cs ₂ CO ₃ /2	100	27
4	10	L1/20	Et ₃ SiH/2	PhMe	Cs ₂ CO ₃ /2	60	75
5	10	L1/20	Et ₃ SiH/2	PhMe	Cs ₂ CO ₃ /2	25	95
6	10	L1/20	Et ₃ SiH/2	CyH	Cs ₂ CO ₃ /2	25	83
7	10	L1/20	Et ₃ SiH/2	1,4-dioxane	Cs ₂ CO ₃ /2	25	94
8	10	L1/20	Et ₃ SiH/2	THF	Cs ₂ CO ₃ /2	25	72
9	10	L2/20	Et ₃ SiH/2	PhMe	Cs ₂ CO ₃ /2	25	<5
10	10	L3/20	Et ₃ SiH/2	PhMe	Cs ₂ CO ₃ /2	25	98
11	10	L3/20	Et ₃ SiH/2	PhMe	Cs ₂ CO ₃ /0.15	25	32
12	10	L3/20	Et ₃ SiH/2	PhMe	Cs ₂ CO ₃ /2	25	<5
13 ^d	5	L3/10	Et ₃ SiH/2	PhMe	Cs ₂ CO ₃ /2	25	96
14	1	L3/2	Et ₃ SiH/2	PhMe	Cs ₂ CO ₃ /2	25	39
15	5	L3/5	Et ₃ SiH/2	PhMe	Cs ₂ CO ₃ /2	25	84

$R^1 = ^i\text{Pr}, R^2 = \text{H}, \text{L1}$
 $R^1 = R^2 = \text{Me}, \text{L2}$
 L3

^aConditions: **1** (0.1 mmol), **2** (0.2 mmol), additive (0.2 mmol), catalyst (10 mol %), ligand (20 mol %), and 1 mL solvent. ^b¹H NMR yield with C₂H₂Cl₄ as an internal standard. ^cTreatment with TBAF. ^dIsolated yield.

C oxidative addition of cyclobutanone. Moreover, the generation of a rigid spironickelacycle intermediate with an endo-cyclic alkene elongates the distance between the nickel center and β -carbon atom, which inhibits strain-release-driven β -carbon elimination. Thus, the realization of this goal will

open a vast opportunity for the strain-storage synthesis of bioisosteric bicyclo[4.1.1] scaffolds (Scheme 1b, left). Beyond strain-storage synthesis, the resulting bicyclo[4.1.1] scaffold could be employed as a strained precursor to undergo transition metal-catalyzed strain-release-driven "cleave and

Scheme 2. Scope of Cyclobutanone-Alkyne Cyclization^{a-c}

^aConditions: **1** (0.2 mmol), **2** (0.4 mmol), Cs_2CO_3 (0.4 mmol), Ni(cod)_2 (5 mol %), **L3** (10 mol %), and 1 mL PhMe, isolated yields. ^bRuphos as a ligand, 80 °C. ^c Ni(cod)_2 (10 mol %), Sphos (20 mol %), PhB(OH)_2 (2 equiv), 100 °C.

resew” transformations (Scheme 1b, right),¹⁹ thus providing a robust platform to expeditiously assemble new structurally diverse 3D molecules. Herein, we report our findings on nickel-catalyzed chemoselective synthesis of strained bicyclo[4.1.1] scaffold via a well-tailored strain-storage oxidative cyclization of cyclobutanones with alkynes, as well as successive rhodium-catalyzed enantioselective ring expansion of strained bicyclo[4.1.1] to deliver challenging enantioenriched bicyclo[4.2.1]nonanes with excellent enantio- and diastereoselectivity.

RESULTS AND DISCUSSION

Following an extensive optimization campaign, we identified the representative conditions outlined in Table 1. By employing Ni(cod)_2 as a catalyst, **L1** as a ligand, triethylsilane as a hydrogen source, cesium carbonate as a base, and toluene as a solvent, we observed a 69% yield of the desired

bicyclo[4.1.1] product upon treatment of TBAF solution (Table 1, entry 1). Other silane surrogates such as bis(pinacolato)diboron and pinacolborane showed a lower efficiency (entries 2 and 3). Lowering reaction temperature to room temperature led to an improved yield, and the desired product was isolated in 95% yield (entries 4 and 5). Further evaluation of other NHC ligands and solvents showed that employing **L3** as a ligand and toluene as a solvent gave optimal reaction efficiency (entries 6–10). Control experiments confirmed the necessity of the ligand and a stoichiometric amount of base in this reaction (entries 11 and 12). We also studied the influence of catalyst loading toward the reactivity. An identical reaction efficiency was observed when the amount of Ni-catalyst was reduced to 5 mol %, while further lowering the catalyst loading to 1 mol % gave a dramatically reduced yield (entries 13 and 14). Finally, a nickel-to-ligand ratio of 1:1

Reaction scheme showing the synthesis of **34** from **10** using $[\text{Rh}(\text{cod})(\text{OH})_2]$ (2.5 mol%) and $(R)\text{-DTBM-SegPhos}$ (6 mol%) in PhMe at 110°C . The reaction proceeds via a $1,4\text{-Rh shift}$ mechanism, as indicated by the dashed box and arrows.

Reaction scheme showing the asymmetric synthesis of a series of chiral sulfonamide derivatives (34-52) using a Rhodium complex and a chiral ligand (L) in the presence of K_2HPO_4 and PhMe at 110 °C.

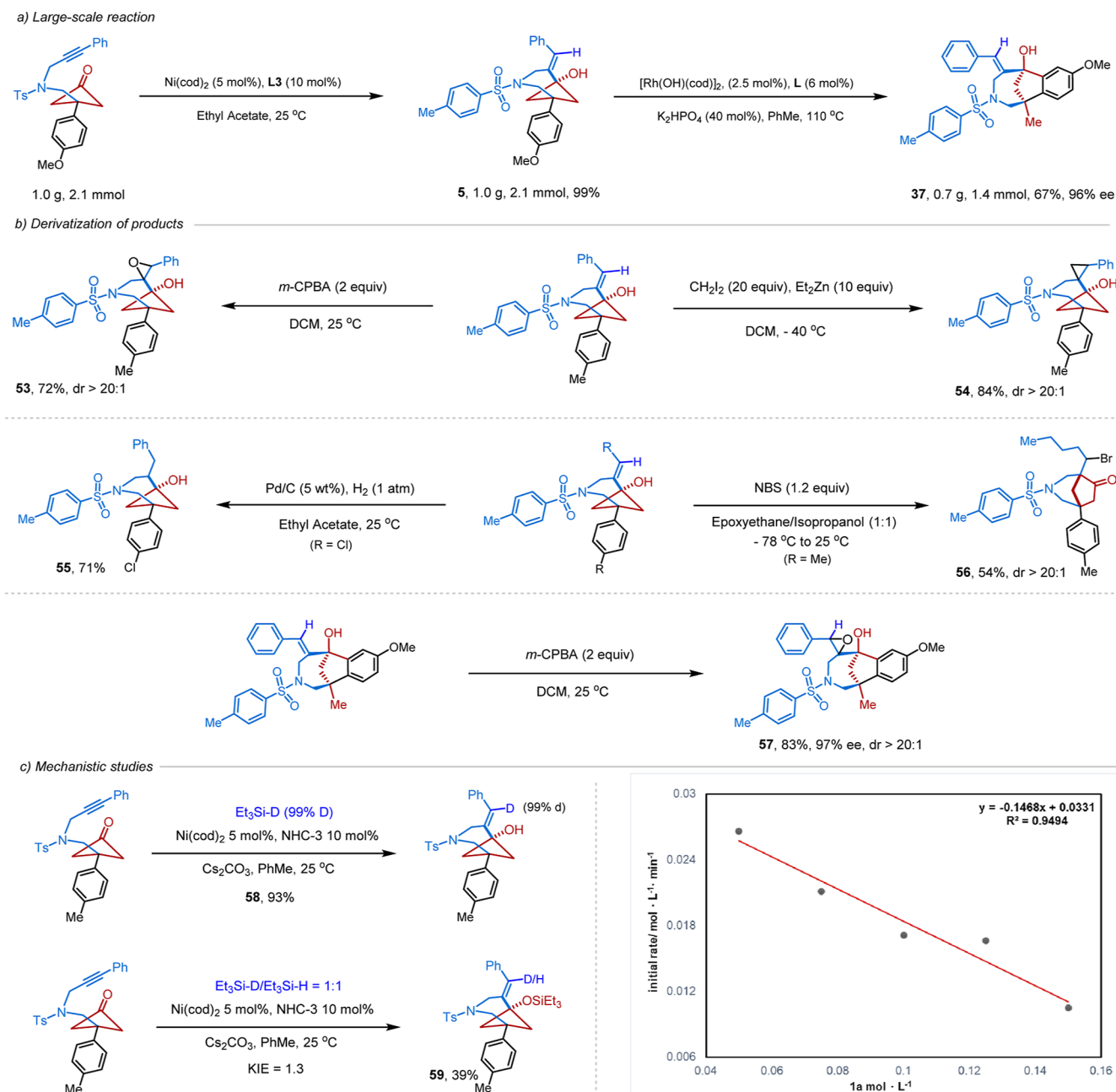
Reaction conditions: $[\text{Rh}(\text{cod})(\text{OH})_2]_2$ (2.5 mol%), L (6 mol%), K_2HPO_4 (40 mol%), PhMe, 110 °C.

Structure of L: L , Ar = DTBM (1,3,5-tri-*t*-butyl-4-methylphenyl).

Yields and enantiomeric excesses (ee) for the products:

- 34, CCDC 2312142
- 35, 84%, 96% ee
- 36, 73%, 90% ee
- 37, 70%, 95% ee
- 38, 96% ee
- 39, 64%, 95% ee
- 40, 56%, 95% ee
- 41, 82%, 95% ee
- 42, 57%, 96% ee
- 43, 93% ee
- 44, 79%, 95% ee
- 45, 67%, 81% ee^[a]
- 46, 80%, 82% ee^[a]
- 47, 45%, 96% ee
- 48, 99% ee
- 49, 61%, 98% ee
- 50, 65%, 98% ee
- 51, 63%, 98% ee
- 52, 57%, 38% ee^[a]

Scheme 5. Derivatization of a Product and Mechanistic Studies

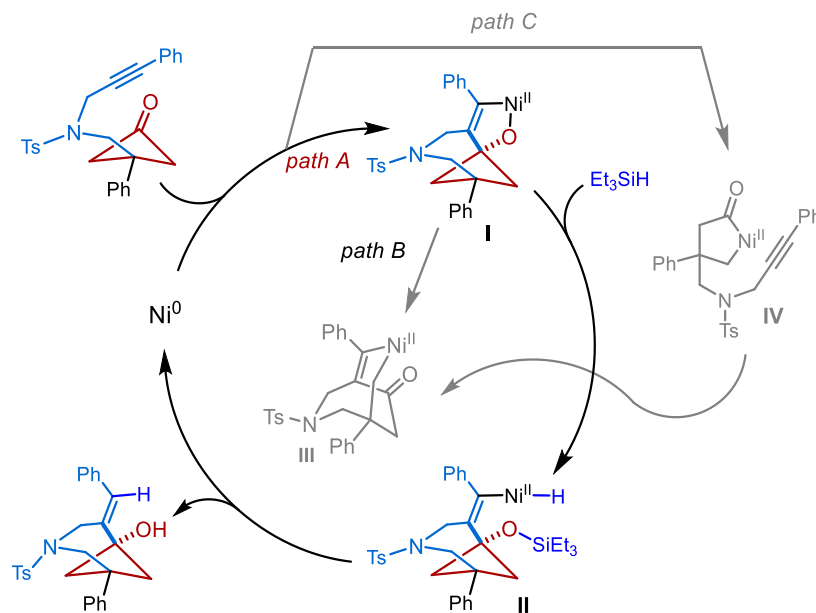


yields. In addition, installing naphthyl (**21**), 4-(trifluoromethyl)phenyl (**22**), 3-(methyl)phenyl (**23**), 3-(methoxy)phenyl (**24**), 5-(methyl)phenyl (**25**), and 5-(methoxy)phenyl (**26**) groups as well as different alkyl groups such as methyl (**27**), ethyl (**28**), *n*-propyl (**29**), and *n*-butyl (**30**) to the alkynyl fragment all underwent the oxidative cyclization smoothly to construct the desired bicyclo[4.1.1] scaffolds in good yields. The coupling of a substrate derived from 1,3-enyne furnished the desired product (**31**) in 87% yield. This example is particularly noteworthy in that the formed 1,3-diene group could coexist well with the excessive triethylsilane, demonstrating the generality of this catalytic system. The reaction of *C*-tethered substrate underwent the cyclization smoothly under the standard conditions, affording the product (**32**) in 88% yield. Beyond triethylsilane, phenylboronic acid is an applicable reagent in this Ni-catalyzed

oxidative cyclization, and the arylated bicyclo[4.1.1] scaffold (**33**) with a tetrasubstituted alkene moiety was prepared in a good yield.

To examine applications of the concept of controllable strain storage and release, we sought to explore synthetically useful strain-release transformations of this strained bicyclo[4.1.1] scaffold. Since seminal works reported by Murakami et al.²⁰ and Seiser and Cramer,²¹ the rhodium-catalyzed enantioselective β -carbon elimination of strained monocyclic alkanol has been an excellent approach for the formation of new monocyclic scaffolds with sterically demanding quaternary stereogenic centers.²² However, enantioselective transformation of strained polycyclic alkanol to construct more complex 3D bicyclic scaffolds remains elusive due to the inherent tedious synthetic procedures and untamable reactivity of the polycyclic molecules.²³ Inspired by our rapid access to

Scheme 6. Proposed Mechanism



bicyclo[4.1.1] scaffold, we envisioned that the sequential rhodium-catalyzed enantioselective β -carbon elimination, stereospecific 1,4-Rh shift, and nucleophilic addition to carbonyl may be an alternative robust strategy for the construction of chiral bicyclo[4.2.1] scaffold, which is a part of biologically active natural compounds such as longifolene and longicamphoric acid (Scheme 3).²⁴ With this conceptual design in mind, we began to examine the rhodium-catalyzed enantioselective strain-release process. After a careful condition screening (see details in the Supporting Information), the optimal conditions to furnish the chiral 3D azabicyclo[4.2.1]-nonanes were established: [Rh(cod)OH]₂ (2.5 mol %), (R)-DTBM-SegPhos (6 mol %), K₂HPO₄ (40 mol %), and PhMe solvent. It is noteworthy that this reaction represents a scarce strategy for chiral bicyclo[4.2.1]nonane skeleton synthesis²⁵ via transition metal asymmetric catalysis.

Under the optimized reaction conditions, the generality of the reaction was then evaluated. As depicted in Scheme 4, substituents including chloro (34), hydrogen atom (35), methyl (36, 39, and 42), and ether group (37, 38, and 40) dioxole (41) at the para, meta, and ortho-positions of aryl rings all underwent the ring expansion process smoothly, giving the bicyclo[4.2.1] products in good yields with excellent diastereo- and enantioselectivities. The absolute configuration of (1*S*, 6*R*)-34 was secured by X-ray crystallographic analysis. The *o*-methylphenyl and *m*-methylphenyl substituents on the alkyne moiety (43 and 44) showed a marginal influence on the reactivity and enantioselectivity. Installation of an *o*-methoxyphenyl or *m*-methoxyphenyl substituent to the alkyne fragment resulted in a reduced reactivity under the standard conditions, while increasing the reaction temperature to 120 °C afforded the desired product in good yield with good enantioselectivity (45 and 46). The substrate with a naphthyl-substituted alkyne (47) also gave the desired product with high enantioselectivity, albeit with a moderate yield due to the increased steric hindrance. The substrates bearing aliphatic alkynes (48–51) were well tolerated, affording the desired products with excellent enantioselectivity. We also examined the rhodium-catalyzed C–C and C–H activation of an

arylated bicyclo[4.1.1] scaffold (33), efficiently generating azabicyclo[4.2.1]nonane 52 in 57% yield with a dramatically reduced enantioselectivity due to the bulky tetrasubstituted alkene fragment. Unfortunately, when performing this rhodium-catalyzed sequential C–C and C–H activation of compound 16, the 1,5-rhodium shift did not occur at the current stage with recovery of the starting material.

The synthetic utility of this transformation is shown in Scheme 5. As shown in Scheme 5a, the nickel-catalyzed cyclization reaction and subsequent rhodium-catalyzed enantioselective ring expansion on a gram scale furnished the corresponding products in good yields. To further demonstrate the applicability of this strategy toward formation of more complex sp³-rich scaffolds, we undertook several useful transformations of bicyclo[4.1.1] product (Scheme 5b). Spirocyclic propagations were performed to access polycyclic skeletons with differently sized rings in high yield with excellent diastereoselectivity via epoxidation (53) or cyclopropanation (54) of the exocyclic alkene of the product. Treatment of the product with hydrogen and Pd/C provided saturated compound 55 in a 71% yield. Transformation into a synthetically useful brominated 3-azabicyclo[3.2.1]octan-6-one skeleton (56) was achieved in 54% yield with excellent diastereoselectivity via NBS-induced semi-pinacol rearrangement. In addition, we performed the oxidation of bicyclo[4.2.1], generating epoxide derivative 57 in 83% yield.

We subsequently performed a series of deuterium-labeling and kinetic experiments to probe the mechanism of this nickel-catalyzed oxidative cyclization process (Scheme 5c). We conducted the cyclization reaction of substrate 1a with Et₃Si-D under standard conditions, and the deuterium atom was located at the alkenyl position. ¹H NMR analysis of the reaction between substrate 1a and a mixture of Et₃Si-D and Et₃Si-H indicated that protonation of alkenyl nickel species is not a rate-determining step due to a small kinetic isotope effect (KIE = 1.3) given in the reaction (Scheme 5c, left). To gain further insight into the process of oxidative cyclization, kinetic analyses were performed. The initial rates of nickel-catalyzed oxidative cyclization were investigated at various concen-

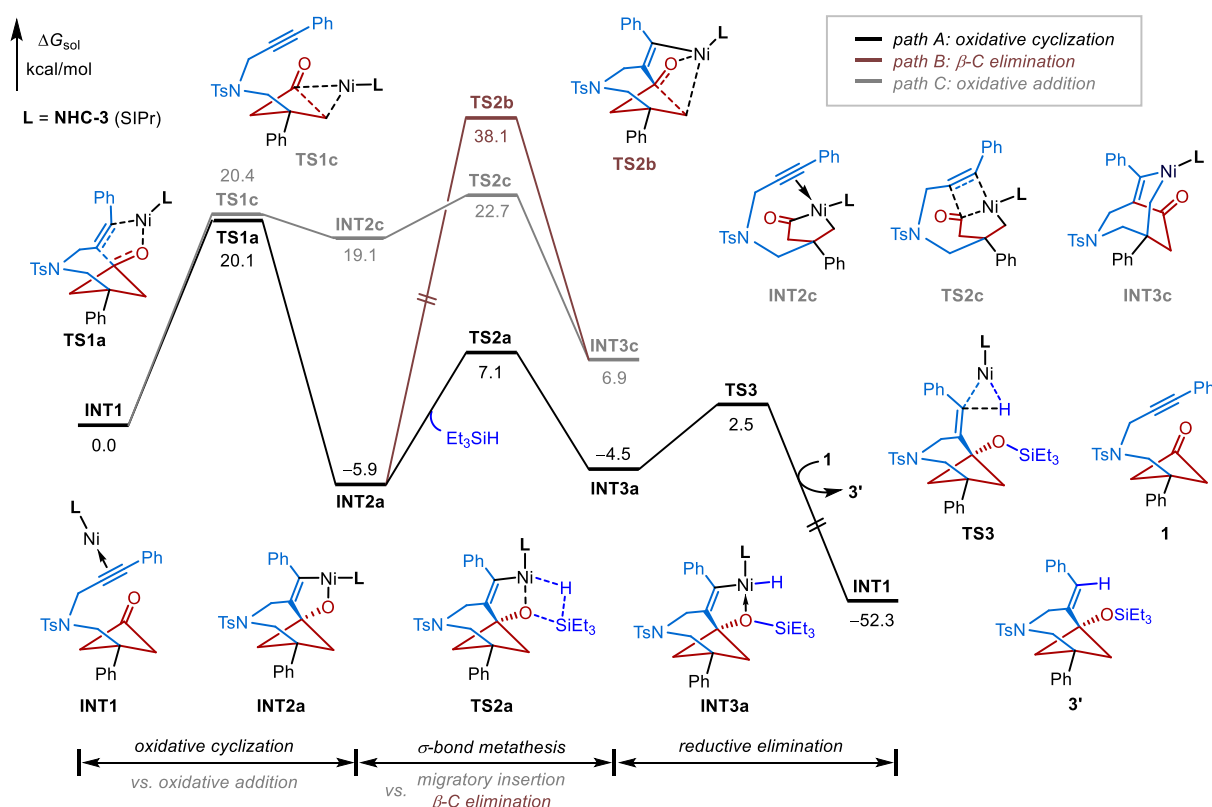


Figure 1. Computed energy profiles for nickel-catalyzed intramolecular annulations of the distally alkynyl-substituted cyclobutanone.

trations of the substrate (Scheme 5c, right). The rates showed a negative first-order dependence on the concentration of substrate **1a**, indicating a strong coordinating interaction between substrate **1a** and the nickel catalyst.

On the basis of previous work²⁶ and our mechanistic studies, possible reaction pathways were proposed as shown in Scheme 6. In path A, the mechanism commences with an oxidative cyclization of alkyne-substituted cyclobutanone with a Ni⁰ catalyst to give rigid bicyclic nickel species **I**, followed by σ -bond metathesis of triethylsilane to generate nickel-hydride species **II**. Reductive elimination provides the desired product and regenerates the Ni⁰ catalyst. Furthermore, two competing strain-release pathways commonly proposed in previous work^{15,16,17a,26} were also considered. The intermediate **I** undergoes β -carbon elimination to generate rigid nickel complex **III** (path B), which was originally proposed in the previous reductive couplings of cyclobutanone with alkyne.¹⁶ Recent DFT calculations all showed that the strain-release-driven oxidative addition of C–C bond to a nickel center to generate a five-membered nickelacycle is energetically superior to the oxidative cyclization process.¹⁷ Thus, in path C, nickel-catalyzed C–C activation of strained cyclobutanone followed by an alkyne insertion to form bicyclic organonickel intermediates **III** was proposed.

After failing isolation of the oxidative cyclization intermediate, DFT calculations were further performed to investigate these competing pathways to unravel the origins of reaction chemoselectivity. The computed energy profiles are shown in Figure 1. Among a series of possible catalyst-substrate complexes, INT1 was identified as the most stable one and chosen as the zero-energy reference (see the details in the Supporting Information). The intramolecular oxidative cyclization between alkynyl and cyclobutanone moieties

requires a barrier of 20.1 kcal/mol (TS1a), forming the spiro-oxa-nickelacycle (INT2a). By reaction with Et₃SiH via σ -bond metathesis (TS2a, $\Delta G^\ddagger = 13.0$ kcal/mol), the Ni–O bond in INT2a is readily cleaved to generate the alkenyl nickel hydride species (INT3a). The ensuing C(alkenyl)–H reductive elimination (TS3) proceeds smoothly to deliver the strained bicyclo[4.1.1] skeleton (3') and regenerate the active catalyst. The relatively low barriers for the steps related to nickel hydride (TS2a and TS3) are in line with both the deuterium-labeling and KIE experimental results (Scheme 5b).

In this strain-storage annulative reaction, the major competing pathways are the undesired strain-release processes. For the spiro-oxa-nickelacycle intermediate (INT2a), the β -carbon elimination is straightforward to release the ring strain. However, this process is less possible due to the extremely high barrier (TS2b, $\Delta G^\ddagger = 44.0$ kcal/mol), which is consistent with prior computational studies of nickel-catalyzed annulations of strained cyclic ketones with π components.¹⁷ The difficulty of β -carbon elimination is mostly because of the great rigidity of the spiro-oxa-nickelacycle (INT2a), which renders the Ni center away from the β -carbon position, bearing a long Ni...C $_{\beta}$ distance (3.76 Å, Figure 2). To approach the β -carbon atom, the alkenyl-Ni moiety in TS2b suffers from significant geometric deformations, which is evidenced by the distorted angle of $\angle C_1C_2Ni$ (from 115° in INT2a to 143° in TS2a, Figure 2). Even after distortions, there is still a relatively long Ni...C $_{\beta}$ distance (2.49 Å) in TS2b, which is unable to effectively stabilize the negatively charged C $_{\beta}$ atom, thus leading to a high barrier. Alternatively, the strain may be released in the initial reaction stage through the oxidative addition of cyclobutanone. Indeed, this oxidative addition requires a relatively low barrier (TS1c, $\Delta G^\ddagger = 20.4$ kcal/mol), which is comparable with that of oxidative cyclization (TS1a,

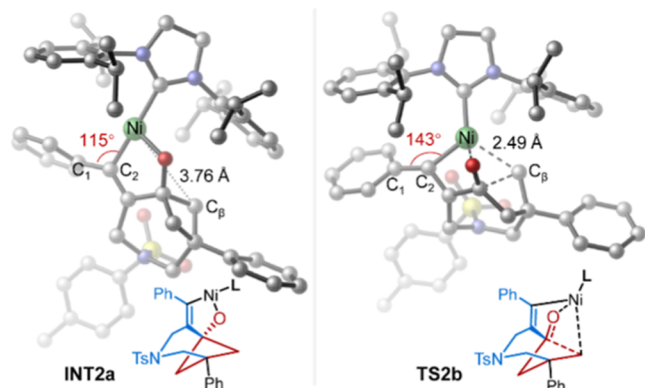


Figure 2. Optimized structures of spiro-oxa-nickelacycle and β -carbon elimination transition state. Hydrogen atoms are omitted for clarity.

$\Delta G^\ddagger = 20.1$ kcal/mol). However, the subsequent alkyne migratory insertion (TS2c, $\Delta G^\ddagger = 22.7$ kcal/mol) is less favorable than that of TS1a. Thus, either at the initial or intermediate stage, the strain-release process is energetically inferior to the strain-retentive pathway. The efficient capture of spiro-oxa-nickelacycle by Et₃SiH is critical for this strain-storage strategy since other silane surrogates (e.g., HBpin) showcased lower efficiency (entries 3, Table 1).

CONCLUSIONS

In summary, we have unveiled a strain-storage approach for the formation of a strained bicyclo[4.1.1] skeleton via formal oxidative cyclization of precisely designed alkyne-substituted cyclobutanones. Mechanistic studies revealed that the rigidity of the nickelacycle generated by oxidative cyclization lengthens the distance between nickel center and β -carbon atom, which hampers the β -C elimination process. Furthermore, the rhodium-catalyzed enantioselective strain-release transformation of bicyclo[4.1.1] skeleton was well-established to generate various synthetically and pharmaceutically useful bicyclo[4.2.1] scaffolds with excellent chemo-, diastereo-, and enantioselectivity. We anticipate that these reactions will be of forceable value to the medicinal chemistry community by assisting the rapid synthesis of highly functionalized 3D bicyclic scaffolds.

ASSOCIATED CONTENT

Supporting Information

The Supporting Information is available free of charge at <https://pubs.acs.org/doi/10.1021/acscatal.5c00065>.

Experimental procedures and physical characterization data (¹H, ¹³C, and ¹⁹F NMR spectra) of the substrates and products (PDF)

AUTHOR INFORMATION

Corresponding Authors

Gang Lu – Institute of Frontier Chemistry, School of Chemistry and Chemical Engineering, Shandong University, Qingdao 266237, China; orcid.org/0000-0002-7319-4315; Email: ganglu@sdu.edu.cn

Xingwei Li – Institute of Frontier Chemistry, School of Chemistry and Chemical Engineering, Shandong University, Qingdao 266237, China; Email: lixw@sdu.edu.cn

Songjie Yu – Institute of Frontier Chemistry, School of Chemistry and Chemical Engineering, Shandong University, Qingdao 266237, China; School of Chemistry, Dalian

University of Technology, Dalian 116024, China;

orcid.org/0000-0001-9156-8774; Email: yusongjie23@sdu.edu.cn

Authors

Hanlin Yang – Institute of Frontier Chemistry, School of Chemistry and Chemical Engineering, Shandong University, Qingdao 266237, China; School of Chemistry, Dalian University of Technology, Dalian 116024, China

Lingfei Hu – Institute of Frontier Chemistry, School of Chemistry and Chemical Engineering, Shandong University, Qingdao 266237, China

Complete contact information is available at:

<https://pubs.acs.org/10.1021/acscatal.5c00065>

Notes

The authors declare no competing financial interest.

ACKNOWLEDGMENTS

We thank the financial support from the National Natural Science Foundation of China (no. 22371029 and 22371171) for financial support. S.Y. thanks the Taishan Scholar of Shandong Province (tsqzn20221108), the Qilu Young Scholar of Shandong University, and the start-up grants of Dalian University of Technology for funding.

REFERENCES

- (1) (a) Lovering, F. Escape from Flatland 2: Complexity and Promiscuity. *MedChemComm* **2013**, *4*, 515–519. (b) Lovering, F.; Bikker, J.; Humblet, C. Escape from Flatland: Increasing Saturation as an Approach to Improving Clinical Success. *J. Med. Chem.* **2009**, *52*, 6752–6756. (c) Mykhailiuk, P. K. Saturated Bioisosteres of Benzene: Where to Go Next? *Org. Biomol. Chem.* **2019**, *17*, 2839–2849.
- (2) (a) Fan, Z.; Strassfeld, D. A.; Park, H. S.; Wu, K.; Yu, J.-Q. Formal γ -C-H Functionalization of Cyclobutyl Ketones: Synthesis of Cis-1,3-Difunctionalized Cyclobutanes. *Angew. Chem., Int. Ed.* **2023**, *62*, No. e202303948. (b) Harmata, A. S.; Spiller, T. E.; Sowden, M. J.; Stephenson, C. R. J. Photochemical Formal (4 + 2)-Cycloaddition of Imine-Substituted Bicyclo[1.1.1]Pentanes and Alkenes. *J. Am. Chem. Soc.* **2021**, *143*, 21223–21228.
- (3) (a) Anderson, J. M.; Measom, N. D.; Murphy, J. A.; Poole, D. L. Bridge Functionalisation of Bicyclo [1.1.1]Pentane Derivatives. *Angew. Chem., Int. Ed.* **2021**, *60*, 24754–24769. (b) He, F.-S.; Xie, S.-M.; Yao, Y.-F.; Wu, J. Recent Advances in the Applications of [1.1.1]Propellane in Organic Synthesis. *Chin. Chem. Lett.* **2020**, *31*, 3065–3072.
- (4) (a) Gianatassio, R.; Lopchuk, J. M.; Wang, J.; Pan, C.-M.; Malins, L. R.; Prieto, L.; Brandt, T. A.; Collins, M. R.; Gallego, G. M.; Sach, N. W.; Spangler, J. E.; Zhu, H.; Baran, P. S. Strain-Release Amination. *Science* **2016**, *351*, 241–246. (b) Kanazawa, J.; Maeda, K.; Uchiyama, M. Radical Multicomponent Carboamination of [1.1.1]Propellane. *J. Am. Chem. Soc.* **2017**, *139*, 17791–17794. (c) Nugent, J.; Arroniz, C.; Shire, B. R.; Sterling, A. J.; Pickford, H. D.; Wong, M. L. J.; Mansfield, S. J.; Caputo, D. F. J.; Owen, B.; Mousseau, J. J.; Duarte, F.; Anderson, E. A. A General Route to Bicyclo[1.1.1]-Pentanes through Photoredox Catalysis. *ACS Catal.* **2019**, *9*, 9568–9574. (d) Zhang, X.; Smith, R. T.; Le, C.; McCarver, S. J.; Shireman, B. T.; Carruthers, N. I.; MacMillan, D. W. C. Copper-Mediated Synthesis of Drug-Like Bicyclopentanes. *Nature* **2020**, *580*, 220–226. (e) Makarov, I. S.; Brocklehurst, C. E.; Karaghiosoff, K.; Koch, G.; Knochel, P. Synthesis of Bicyclo[1.1.1]Pentane Bioisosteres of Internal Alkynes and Para-Disubstituted Benzenes from [1.1.1]-Propellane. *Angew. Chem., Int. Ed.* **2017**, *56*, 12774–12777. (f) Huang, W.; Keess, S.; Molander, G. A. A General and Practical Route to Functionalized Bicyclo[1.1.1]Pentane-Heteroaryls Enabled by Photocatalytic Multicomponent Heteroarylation of [1.1.1]-

- Propellane. *Angew. Chem., Int. Ed.* **2023**, 62, No. e202302223. (g) Yu, S.; Jing, C.; Noble, A.; Aggarwal, V. K. Iridium-Catalyzed Enantioselective Synthesis of α -Chiral Bicyclo[1.1.1]Pentanes by 1,3-Difunctionalization of [1.1.1] Propellane. *Org. Lett.* **2020**, 22, 5650–5655. (h) Wu, Z.; Xu, Y.; Liu, J.; Wu, X.; Zhu, C. A Practical Access to Fluoroalkylthio(Seleno)-Functionalized Bicyclo[1.1.1]-Pentanes. *Sci. China Chem.* **2020**, 63, 1025–1029.
- (5) (a) Kleinmans, R.; Pinkert, T.; Dutta, S.; Paulisch, T. O.; Keum, H.; Daniliuc, C. G.; Glorius, F. Intermolecular $[2\pi+2\sigma]$ -Photocycloaddition Enabled by Triplet Energy Transfer. *Nature* **2022**, 605, 477–482. (b) Agasti, S.; Beltran, F.; Pye, E.; Kaltsoyannis, N.; Crisenza, G. E. M.; Procter, D. J. A Catalytic Alkene Insertion Approach to Bicyclo[2.1.1]Hexane Bioisosteres. *Nat. Chem.* **2023**, 15, 535–541. (c) Xu, M.; Wang, Z.-J.; Sun, Z.-H.; Ouyang, Y.-Z.; Ding, Z.-W.; Yu, T.; Xu, L.; Li, P.-F. Diboron(4)-Catalyzed Remote $[3+2]$ Cycloaddition of Cyclopropanes Via Dearomative/Rearomative Radical Transmission through Pyridine. *Angew. Chem., Int. Ed.* **2022**, 61, No. e202214507. (d) Guo, R.; Chang, Y.-C.; Herter, L.; Salome, C.; Braley, S. E.; Fessard, T. C.; Brown, M. K. Strain-Release $[2\pi+2\sigma]$ Cycloadditions for the Synthesis of Bicyclo[2.1.1]Hexanes Initiated by Energy Transfer. *J. Am. Chem. Soc.* **2022**, 144, 7988–7994. (e) Liu, Y.; Lin, S.; Li, Y.; Xue, J.-H.; Li, Q.; Wang, H. Pyridine-Boryl Radical-Catalyzed $[2\pi+2\sigma]$ Cycloaddition of with Alkenes. *ACS Catal.* **2023**, 13, 5096–5103. (f) Liang, Y.; Kleinmans, R.; Daniliuc, C. G.; Glorius, F. Synthesis of Polysubstituted 2-Oxabicyclo[2.1.1]-Hexanes Via Visible- Light-Induced Energy Transfer. *J. Am. Chem. Soc.* **2022**, 144, 20207–20213. (g) Tang, L.; Xiao, Y.; Wu, F.; Zhou, J.-L.; Xu, T.-T.; Feng, J.-J. Silver-Catalyzed Dearomative $[2\pi+2\sigma]$ Cycloadditions of Indoles with Bicyclobutanes: Access to Indoline Fused Bicyclo[2.1.1]Hexanes. *Angew. Chem., Int. Ed.* **2023**, 62, No. e202310066.
- (6) (a) Frank, N.; Nugent, J.; Shire, B. R.; Pickford, H. D.; Rabe, P.; Sterling, A. J.; Zarganes-Tzitzikas, T.; Grimes, T.; Thompson, A. L.; Smith, R. C.; Schofield, C. J.; Brennan, P. E.; Duarte, F.; Anderson, E. A. Synthesis of Meta-Substituted Arene Bioisosteres from [3.1.1]-Propellane. *Nature* **2022**, 611, 721–726. (b) Zheng, Y.; Huang, W.; Dhungana, R. K.; Granados, A.; Keess, S.; Makvandi, M.; Molander, G. A. Photochemical Intermolecular $[3\sigma+2\sigma]$ -Cycloaddition for the Construction of Aminobicyclo[3.1.1]Heptanes. *J. Am. Chem. Soc.* **2022**, 144, 23685–23690. (c) Zhang, X.-G.; Zhou, Z.-Y.; Li, J.-X.; Chen, J.-J.; Zhou, Q.-L. Copper-Catalyzed Enantioselective $[4\pi+2\sigma]$ Cycloaddition of Bicyclobutanes with Nitrones. *J. Am. Chem. Soc.* **2024**, 146, 27274–27281. (d) Lin, Z.; Ren, H.; Lin, X.; Yu, X.; Zheng, J. Synthesis of Azabicyclo[3.1.1]Heptenes Enabled by Catalyst-Controlled Annulations of Bicyclo[1.1.0]Butanes with Vinyl Azides. *J. Am. Chem. Soc.* **2024**, 146, 18565–18575. (e) Yu, T.; Yang, J.; Wang, Z.; Ding, Z.; Xu, M.; Wen, J.; Xu, L.; Li, P. Selective $[2\sigma+2\sigma]$ Cycloaddition Enabled by Boronyl Radical Catalysis: Synthesis of Highly Substituted Bicyclo[3.1.1]Heptanes. *J. Am. Chem. Soc.* **2023**, 145, 4304–4310.
- (7) Wang, H.; Shao, H.; Das, A.; Dutta, S.; Chan, H. T.; Daniliuc, C.; Houk, K. N.; Glorius, F. Dearomative Ring Expansion of Thiophenes by Bicyclobutane Insertion. *Science* **2023**, 381, 75–81.
- (8) Nicolai, S.; Waser, J. Lewis Acid Catalyzed $[4+2]$ Annulation of Bicyclobutanes with Dienol Ethers for the Synthesis of Bicyclo[4.1.1]-Octanes. *Chem. Sci.* **2024**, 15, 10823–10829.
- (9) (a) Yu, S.; Ai, Y.; Hu, L.; Lu, G.; Duan, C.; Ma, Y. Palladium-Catalyzed Stagewise Strain-Release-Driven C-C Activation of Bicyclo[1.1.1]Pentanyl Alcohols. *Angew. Chem., Int. Ed.* **2022**, 61, No. e202200052. (b) Fu, Z.; Cheng, J.; Li, X.-X.; Li, X.; Yu, S. Gem-Difluorobicyclo[2.1.1]Hexanes Via Photochemical $[2\pi+2\sigma]$ Cycloaddition Initiated by Oxidative Activation of Gem-Difluorodienes. *Org. Lett.* **2024**, 26, 9961–9966. (c) Liu, H.; Fu, Z.; Li, X.; Yu, S. Halogen-bond-assisted radical remote difunctionalization of bicyclo[1.1.1]butane skeleton. *Green Chem.* **2024**, 27, 256–263.
- (10) (a) Wender, P. A.; Correa, A. G.; Sato, Y.; Sun, R. Transition Metal-Catalyzed $[6+2]$ Cycloadditions of 2-Vinylcyclobutanones and Alkenes: A New Reaction for the Synthesis of Eight-Membered Rings. *J. Am. Chem. Soc.* **2000**, 122, 7815–7816. (b) Kondo, T.; Taguchi, Y.; Kaneko, Y.; Niimi, M.; Mitsudo, T. A Ru- and Rh-Catalyzed C-C Bond Cleavage of Cyclobutenones: Reconstructive and Selective Synthesis of 2-Pyranones, Cyclopentenones, and Cyclohexenones. *Angew. Chem., Int. Ed.* **2004**, 43, 5369–5372. (c) Matsuda, T.; Shigeno, M.; Murakami, M. Asymmetric Synthesis of 3,4-Dihydrocoumarins by Rhodium-Catalyzed Reaction of 3-(2-Hydroxyphenyl)Cyclobutanones. *J. Am. Chem. Soc.* **2007**, 129, 12086–12087. (d) Soullart, L.; Parker, E.; Cramer, N. Highly Enantioselective Rhodium(I)-Catalyzed Activation of Enantiotopic Cyclobutanone C-C Bonds. *Angew. Chem., Int. Ed.* **2014**, 53, 3001–3005.
- (11) (a) Zhang, G.-Y.; Zhang, P.; Li, B.-W.; Liu, K.; Li, J.; Yu, Z.-X. Dual Activation Strategy to Achieve C-C Cleavage of Cyclobutanones: Development and Mechanism of Rh and Zn Cocatalyzed $[4+2]$ Cycloaddition of Yne-Vinylcyclobutanones. *J. Am. Chem. Soc.* **2022**, 144, 21457–21469. (b) Murakami, M.; Ashida, S.; Matsuda, T. Nickel-Catalyzed Intermolecular Alkyne Insertion into Cyclobutanones. *J. Am. Chem. Soc.* **2005**, 127, 6932–6933. (c) Julia-Hernandez, F.; Ziadi, A.; Nishimura, A.; Martin, R. Nickel-Catalyzed Chemo-Regio- and Diastereoselective Bond Formation through Proximal C-C Cleavage of Benzocyclobutenones. *Angew. Chem., Int. Ed.* **2015**, 54, 9537–9541. (d) Kumar, P.; Zhang, K.; Louie, J. An Expedient Route to Eight-Membered Heterocycles by Nickel-Catalyzed Cycloaddition: Low-Temperature C_{sp^2} - C_{sp^3} Bond Cleavage. *Angew. Chem., Int. Ed.* **2012**, 51, 8602–8606.
- (12) Zhou, X.; Dong, G. $(4+1)$ Vs $(4+2)$: Catalytic Intramolecular Coupling between Cyclobutanones and Trisubstituted Allenes Via C-C Activation. *J. Am. Chem. Soc.* **2015**, 137, 13715–13721.
- (13) (a) Ko, H. M.; Dong, G. Cooperative Activation of Cyclobutanones and Olefins Leads to Bridged Ring Systems by a Catalytic $[4+2]$ Coupling. *Nat. Chem.* **2014**, 6, 739–744. (b) Zhou, X.; Ko, H. M.; Dong, G. Synthesis of Bridged Cyclopentane Derivatives by Catalytic Decarbonylative Cycloaddition of Cyclobutanones and Olefins. *Angew. Chem., Int. Ed.* **2016**, 55, 13867–13871. (c) Hou, S.-H.; Yu, X.; Zhang, R.; Deng, L.; Zhang, M.; Prichina, A. Y.; Dong, G. Enantioselective Type II Cycloaddition of Alkynes Via C-C Activation of Cyclobutanones: Rapid and Asymmetric Construction of [3.3.1] Bridged Bicycles. *J. Am. Chem. Soc.* **2020**, 142, 13180–13189.
- (14) (a) Ma, J.; Duan, J.; Yu, Z.-X. Ni(0)-Catalyzed Rearrangement of Vinylcyclobutanones (Vcbos) to Synthesize Six-Membered Non-Conjugated Enones. *Angew. Chem., Int. Ed.* **2024**, 64 (6), No. e202417407. (b) Thakur, A.; Facer, M. E.; Louie, J. Nickel-Catalyzed Cycloaddition of 1,3-Dienes with 3-Azetidinones and 3-Oxetanones. *Angew. Chem., Int. Ed.* **2013**, 52, 12161–12165. (c) Liu, L.; Ishida, N.; Murakami, M. Atom- and Step-Economical Pathway to Chiral Benzobicyclo [2.2.2] Octenones through Carbon-Carbon Bond Cleavage. *Angew. Chem., Int. Ed.* **2012**, 51, 2485–2488. (d) Saito, N.; Sugimura, Y.; Sato, Y. A Facile Construction of Bi- or Tricyclic Skeletons by Nickel-Catalyzed Stereoselective Cyclization of Alkynylcycloalkane. *Org. Lett.* **2010**, 12, 3494–3497.
- (15) Zhou, X.; Dong, G. Nickel-Catalyzed Chemo- and Enantioselective Coupling between Cyclobutanones and Allenes: Rapid Synthesis of [3.2.2] Bicycles. *Angew. Chem., Int. Ed.* **2016**, 55, 15091–15095.
- (16) (a) Chen, P.-h.; Billett, B. A.; Tsukamoto, T.; Dong, G. Cut and Sew Transformations Via Transition-Metal-Catalyzed Carbon-Carbon Bond Activation. *ACS Catal.* **2017**, 7, 1340–1360. (b) Murakami, M.; Ishida, N. Cleavage of Carbon-Carbon σ -Bonds of Four-Membered Rings. *Chem. Rev.* **2021**, 121, 264–299.
- (17) (a) Li, J.; Luo, J.; Tong, W.; Tang, D.; Zhang, J.; Zhang, Z.-H.; Qu, S. Mechanistic Study of Nickel-Catalyzed Intramolecular $[4+2]$ Cycloaddition of Cyclobutanone with Allene: Origin of Selectivity and Ligand Effect. *Org. Chem. Front.* **2023**, 10, 1134–1146. (b) Li, Y.; Lin, Z. Theoretical Studies on Nickel-Catalyzed Cycloaddition of 3-Azetidinone with Alkynes. *Organometallics* **2013**, 32, 3003–3011. (c) Zou, H.; Wang, Z.-L.; Huang, G. Mechanism and Origins of the Chemo- and Regioselectivities in Nickel-Catalyzed Intermolecular

Cycloadditions of Benzocyclobutenones with 1,3-Dienes. *Chem.—Eur. J.* **2017**, *23*, 12593–12603.

(18) (a) Standley, E. A.; Tasker, S. Z.; Jensen, K. L.; Jamison, T. F. Nickel Catalysis: Synergy between Method Development and Total Synthesis. *Acc. Chem. Res.* **2015**, *48*, 1503–1514. (b) Zhang, Y.-Q.; Hu, L.; Yuwen, L.; Lu, G.; Zhang, Q.-W. Nickel-Catalyzed Enantioselective Hydrosulfenation of Alkynes. *Nat. Catal.* **2023**, *6*, 487–494.

(19) (a) Wang, Y.; Qiu, B.; Hu, L.; Lu, G.; Xu, T. Rh-Catalyzed Cascade C-C/C_{olefin}-H Activations and Mechanistic Insight. *ACS Catal.* **2021**, *11*, 9136–9142. (b) Cao, J.; Xu, L.-W. Palladium- and Nickel-Catalyzed Cascade Enantioselective Ring-Opening/Coupling Reactions of Cyclobutanones. *Chem. Commun.* **2023**, *59*, 3373–3382. (c) Deng, L.; Jin, L.; Dong, G. Fused-Ring Formation by an Intramolecular “Cut-and-Sew” Reaction between Cyclobutanones and Alkynes. *Angew. Chem., Int. Ed.* **2018**, *57*, 2702–2706. (d) Li, X.; Hu, L.; Ma, S.; Yu, H.; Lu, G.; Xu, T. Divergent Rh Catalysis: Asymmetric Dearomatization Versus C-H Activation Initiated by C-C Activation. *ACS Catal.* **2023**, *13*, 4873–4881.

(20) Murakami, M.; Itahashi, T.; Ito, Y. Catalyzed Intramolecular Olefin Insertion into a Carbon-Carbon Single Bond. *J. Am. Chem. Soc.* **2002**, *124*, 13976–13977.

(21) Seiser, T.; Cramer, N. Enantioselective C-C Bond Activation of Allenyl Cyclobutanes: Access to Cyclohexenones with Quaternary Stereogenic Centers. *Angew. Chem., Int. Ed.* **2008**, *47*, 9294–9297.

(22) (a) Seiser, T.; Cramer, N. Rhodium-Catalyzed C-C Bond Cleavage: Construction of Acyclic Methyl Substituted Quaternary Stereogenic Centers. *J. Am. Chem. Soc.* **2010**, *132*, 5340–5341. (b) Lu, J.; Zhang, M.; Zheng, X.; Shen, P.; Xu, Y.; Zhang, Q.; Tang, Y.; Zhang, G.; Guo, R. Rhodium(I)-Catalyzed Enantioselective Ring-Opening and Isomerization of Cyclobutanols through a (Z)-Unsaturated Ketone Intermediate. *Org. Lett.* **2023**, *25*, 5151–5156. (c) Zheng, X.; Guo, R.; Zhang, G.; Zhang, D. Rhodium(I)-Catalyzed Asymmetric [4 + 2] Cycloaddition Reactions of 2-Alkylencyclobutanols with Cyclic Enones through C-C Bond Cleavage: Efficient Access to Trans-Bicyclic Compounds. *Chem. Sci.* **2018**, *9*, 1873–1877. (d) Ishida, N.; Necas, D.; Masuda, Y.; Murakami, M. Enantioselective Construction of 3-Hydroxypiperidine Scaffolds by Sequential Action of Light and Rhodium Upon N-Allylglyoxylamides. *Angew. Chem., Int. Ed.* **2015**, *54*, 7418–7421.

(23) (a) Na, C. G.; Kang, S. H.; Sarpong, R. Development of a C-C Bond Cleavage/Vinylation/Mizoroki-Heck Cascade Reaction: Application to the Total Synthesis of 14- and 15-Hydroxypatchoulol. *J. Am. Chem. Soc.* **2022**, *144*, 19253–19257. (b) Leger, P. R.; Kuroda, Y.; Chang, S.; Jurczyk, J.; Sarpong, R. C-C Bond Cleavage Approach to Complex Terpenoids: Development of a Unified Total Synthesis of the Phomactins. *J. Am. Chem. Soc.* **2020**, *142*, 15536–15547. (c) Ham, J. S.; Park, B.; Son, M.; Roque, J. B.; Jurczyk, J.; Yeung, C. S.; Baik, M.-H.; Sarpong, R. C-H/C-C Functionalization Approach to N-Fused Heterocycles from Saturated Azacycles. *J. Am. Chem. Soc.* **2020**, *142*, 13041–13050. (d) Kerschgens, I.; Rovira, A. R.; Sarpong, R. Total Synthesis of (–)-Xishacorene B from (R)-Carvone Using a C-C Activation Strategy. *J. Am. Chem. Soc.* **2018**, *140*, 9810–9813.

(24) Kadikova, G. N.; Dzhemileva, L. U.; D'Yakonov, V. A.; Dzhemilev, U. M. Synthesis of Functionally Substituted Bicyclo[4.2.1]Nona-2,4-Dienes and Bicyclo[4.2.1]Nona-2,4,7-Trienes by Cobalt(I)-Catalyzed [6 π +2 π] Cycloaddition of 2-Tropylcyclohexanone. *ACS Omega* **2020**, *5*, 31440–31449.

(25) Zhao, J.; Zheng, X.; Gao, Y.-S.; Mao, J.; Wu, S.-X.; Yang, W.-L.; Luo, X.; Deng, W.-P. Organocatalytic Enantioselective [8 + 4] Cycloadditions of Isobenzofulvenes for the Construction of Bicyclo[4.2.1]Nonanes. *Chin. J. Chem.* **2021**, *39*, 3219–3224.

(26) (a) Oblinger, E.; Montgomery, J. A New Stereoselective Method for the Preparation of Allylic Alcohols. *J. Am. Chem. Soc.* **1997**, *119*, 9065–9066. (b) Fu, W.; Nie, M.; Wang, A.; Cao, Z.; Tang, W. Highly Enantioselective Nickel-Catalyzed Intramolecular Reductive Cyclization of Alkynones. *Angew. Chem., Int. Ed.* **2015**, *54*, 2520–2524. (c) McCarren, P. R.; Liu, P.; Cheong, P. H.-Y.; Jamison, T. F.; Houk, K. N. Mechanism and Transition-State Structures for Nickel-

Catalyzed Reductive Alkyne-Aldehyde Coupling Reactions. *J. Am. Chem. Soc.* **2009**, *131*, 6654–6655. (d) Yang, Y.; Zhu, S.-F.; Zhou, C.-Y.; Zhou, Q.-L. Nickel-Catalyzed Enantioselective Alkylative Coupling of Alkynes and Aldehydes: Synthesis of Chiral Allylic Alcohols with Tetrasubstituted Olefins. *J. Am. Chem. Soc.* **2008**, *130*, 14052–14053. (e) Tang, X. Q.; Montgomery, J. Nickel-Catalyzed Preparation of Bicyclic Heterocycles: Total Synthesis of (+)-Allopumiliotoxin 267a, (+)-Allopumiliotoxin 339a, and (+)-Allopumiliotoxin 339b. *J. Am. Chem. Soc.* **2000**, *122*, 6950–6954.